A Note on Feature Selection for Polyp Detection in CT Colonography

Tarik A. Chowdhury, Ovidiu Ghita, Paul F. Whelan and Abhilash Miranda
Vision Systems Group
School of Electronic Engineering
Dublin City University, Dublin 9, Ireland
{tarik,ghitao,whelanp,abhilash}@eeng.dcu.ie

Abstract

In this paper we describe a computer aided detection (CAD) algorithm for robust detection of polyps in computed tomography (CT) colonography. The devised algorithm identifies suspicious polyp candidate surfaces using the surface normal intersection, Hough transform, 3D histogram analysis, region growing and a convexity test. From these detected surfaces we extract statistical and morphological features in order to evaluate if the surface in question is a polyp or fold. In order to devise the optimal classification scheme the performance of two different classifiers are evaluated when the algorithm is applied to synthetic and real patient data. The experimental results indicate that the overall polyp detection performance shows sensitivity higher than 92% for polyps larger than 5mm with an average of 4.7 to 6.0 false positives per dataset.

1. Introduction

Computed Tomography Colonography (CTC) [1,2] is a rapidly evolving technique for early detection of colonic polyps. It provides the interactive evaluation in two dimensional (2D) and three dimensional (3D) views of the data acquired from modern *CT* scanners and many medical practitioners have considered the *CTC* as the optimal mass screening technique for colorectal cancer [3]. Although *CTC* is a relatively new medical investigation technique, a significant number of studies have been conducted to evaluate its performance and as a result a large number of different automated computer aided detection (CAD) techniques have emerged. In this regard, Vinning et al. [4] employed curvature analysis to detect potential colonic polyps and their method achieved 73% sensitivity with 9 to 90 false positives (FP)/dataset. A related technique has been developed by Summers et al. [5] where the convexity of the colonic wall was evaluated by calculating the partial derivatives that are used in conjunction with some local shape criteria. The sensitivity of their technique varied between 29% to 100% with 6 to 20 false positives per dataset. This method has been advanced by Yoshida et al. [6] by developing a technique that uses features such as the shape index and local curvature calculated from small volumes of interest that were used as inputs for a fuzzy clustering in order to discriminate between polyps and folds. They reported 89% sensitivity with 2 false positives (FP) per dataset. Paik et al. [7] proposed a different approach for polyp identification where they evaluated the local convexity of the colonic wall using the normal intersection. This method was efficient to detect polyps but the level of false positives was high. To address this issue Kiss et al. [8] augmented the normal intersection with sphere fitting to produce 85% polyp sensitivity for polyps larger than 6mm with 2.82 FP/dataset.

In this paper we propose a method for polyp detection where we try to maximally exploit the difference in morphology between polyps and folds. In the development of this technique we have used the knowledge that polyps resemble spherical/ellipsoid structures whereas folds have generally cylindrical shapes. It is worth noting that the polyps and folds have almost an unbounded range of shapes and the difference in their appearance is sometimes very subtle. With this in mind, to evaluate the morphology of polyps and folds we calculate the surface change behavior (SCB) with respect to their centers. To determine the *SCB*, the 3dB point, the standard deviation of the surface change, maximum distance and surface normal concentration have been calculated. These features were employed to determine whether a candidate surface is a polyp or not and two classification schemes were evaluated in order to find which classifier performs best in reducing the number of false positives.

2. Colon Lumen Segmentation

Initially the non-isotropic patient data was converted to isotropic by using cubic interpolation. As the *CTC* images offer a good contrast between the gaseous and lean tissue

the colon can be successfully segmented by using a standard seeded region-growing algorithm [9]. Sometimes remaining residual material and water can create collapses in the colon and the region-growing algorithm may require multiple seed points to segment the entire colon. The threshold value for segmentation was set to -800HU and the colon wall (CW) is determined by the voxels situated on the vicinity of the data segmented by the region-growing algorithm that has an *HU* value higher than -800HU.

2.1. Initial candidate surface identification

The candidate surfaces were extracted based on the observation that the surfaces that define polyps are convex. To evaluate the convexity index we developed a detection method based on surface normal intersection, Hough transform and 3D histogram analysis. The normal vector to each colonic wall voxel was calculated using the partial derivatives that are calculated in the x, y, z directions [10]. Once the normal vectors are calculated for each *CW* voxel, the intersections between normal vectors in 3D are evaluated. In this way, each *CW* voxel generates 8 Hough points (HP) along the normal direction starting from 2.0mm to 10.0 mm and their intersections are recorded in a 3D histogram. If the input surface is convex it has a large number of intersections in the 3D histogram for one point between 2.0mm and 10.0mm.

In our implementation we examined whether the 3D histogram of the Hough points has bins with more than 5 intersections. If this is the case, the bin with highest number of intersections will generate the initial candidate center point (ICCP) for a polyp.

The center for each *HP* cluster that defines an initial candidate surface is calculated using the Gaussian distribution illustrated in Eq. 1

$$GM_i = \sum_{k=1}^{M} e^{(-x^2/2.0\times\sigma)} \qquad (1)$$

were x is the distance between the Hough points, σ is the standard deviation and is set to 1.0, M is the number of Hough points in the cluster i and k takes values between 1 to M. The *HP* with the highest distribution is considered to be the center of the clustered surface.

3. Features Extraction

Our objective is to extract features from the candidate surfaces that offer the best discrimination between polyps and folds. At this stage it is useful to recall that polyps and folds have various shapes and in some situations the difference between them is subtle. Thus, the discriminative features employed have to optimally exploit the difference in morphology between polyps and folds in order to achieve robust polyp identification and low level of false positives. In this regard, we extracted the maximum distance from the cluster center to the surface normal, the standard deviation (SD) of the surface variation, the 3-decibel (dB) point on the surface change curve and the surface number concentration. In the remainder of this section we will present these features in detail.

3.1. Maximum distance calculation

The nominal shape for a polyp is spherical/ellipsoid and cylindrical for folds. Thus, the maximum distance between the center of the candidate surface and normal vectors of the candidate surface shows a good discriminative power in separating spherical surfaces from cylindrical surfaces. In this regard the maximal distance should be significantly higher if the candidate surface belongs to a fold than in cases when they belong to polyps. This can be clearly observed in Fig 1. where the maximum distance d_{max} is plotted for different classes of polyps and folds. From Fig. 1 we can notice that this feature is effective in discriminating small/medium polyps ($< 10mm$) when compared to folds. The maximum distance d_{max} does not provide optimal discrimination when the size of the polyp is higher than 10mm (see the plot for class polyp 3).

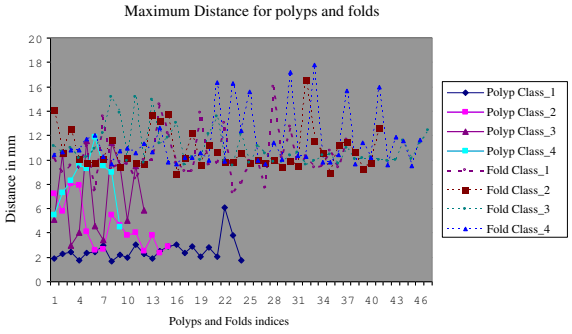

Figure 1. Maximum distance d_{max} for different classes of polyps and folds (classes are sorted in ascending order with respect to the size of the polyps/ folds)

3.2. Standard deviation (SD) of the surface variation

The aim of this feature is to evaluate the rate of surface change. In order to evaluate the standard deviation (SD) of the candidate surface we calculate the number of surface voxels that are placed at each radius starting from d_{max} towards the minimum radius that was set to 1mm. Our goal is

to determine how many voxels from the candidate surfaces are situated at a particular distance with respect to the distance center, this will generate the surface number *SN*. The equations required to calculate the surface number SN_j for each radius are illustrated in Eqns. 2 to 4, where N is the number of steps required to sample the surface curvature.

$$Step = (d_{max} - 1.0)/N \tag{2}$$

$$R_j = d_{max} - Step \times j \qquad for \quad j = 1, ..., N, \tag{3}$$

$$SN_j = \sum_{R_j} Voxel \tag{4}$$

Figs. 2 and 3 illustrate the voxel distribution with respect to each radius R_j for different classes of polyps and folds. From these images it can be observed that the number of

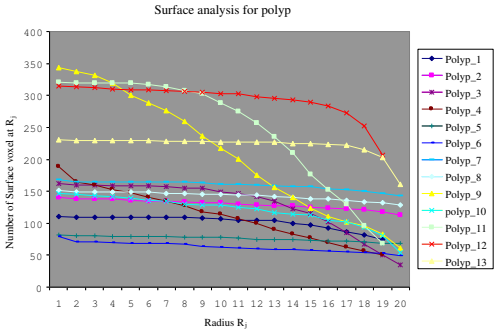

Figure 2. Number of surface voxels for each radius (R_j) for polyp classes.

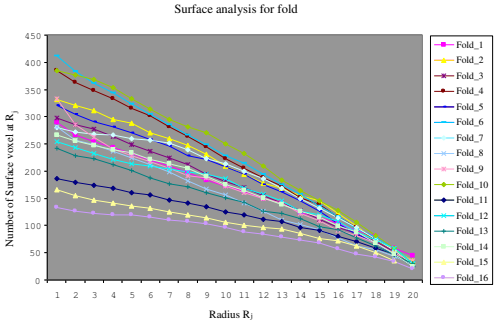

Figure 3. Number of surface voxels for each radius (R_j) for fold classes.

voxels for folds decrease rapidly while for polyps it is almost constant. Thus the surface number can be used to determine the change in curvature and this is best sampled by the standard deviation (SD) that is calculated as illustrated in Eqns. 5 to 7.

$$SN_{jmean} = \frac{1}{N} \sum_{j=1}^{N} SN_j \tag{5}$$

$$SN_{jnorm} = \frac{SN_j}{SN_{jmean}} \qquad for \quad j = 1, ..., N, \tag{6}$$

$$SN_{SD} = \sqrt{\frac{1}{N} \sum_{j=1}^{N} (SN_{jnorm} - SN_{jmean})^2} \tag{7}$$

The discrimination offered by the standard deviation (SD) of the surface variation for different classes of polyps and folds is depicted in Fig. 4. It can be observed that this feature is quite effective in discriminating polyps from all types of folds.

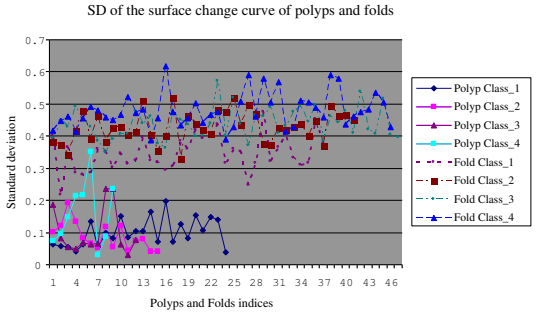

Figure 4. Standard deviation of the surface variation for different classes of polyps and folds (classes are sorted in ascending order with respect to the size of the polyps/ folds)

3.3. 3dB point on surface change curve

The 3dB point refers to the number of steps required by the SN_j to reach the 3 dB ($3dB = \sum_{j=1}^{N} SN_j/\sqrt{2}$) fall in the total voxel count of the candidate surface The number of steps required to reach the 3dB point is generally higher for polyps than for folds and this is illustrated in Fig. 5.

3.4. Surface normal concentration

We recall that for each *CW* voxel we created 8 HP's uniformly distributed along the normal direction from 2.0mm to 10.0mm and the Gaussian distribution has been employed to determine the surface center. The normal concentration is given by the number of surface points that generate an intersection within 1.25mm from the calculated surface center. As the shape of polyps resembles a spherical surface is expected that the surface normal concentration to

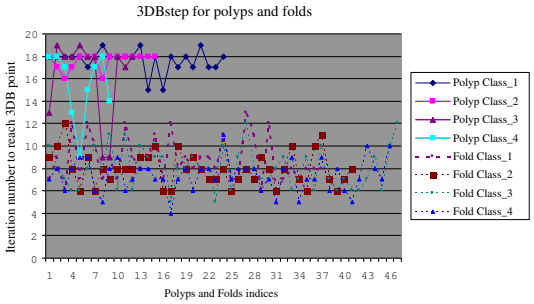

Figure 5. The number of steps required in reaching the 3dB point on surface change for different classes of polyps and folds.

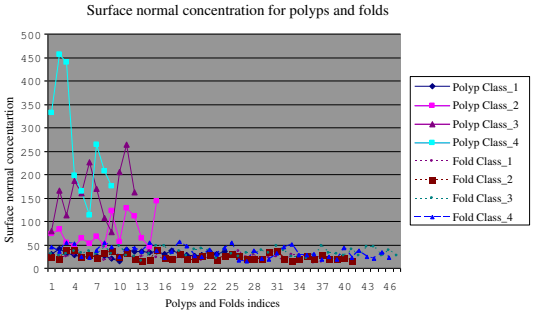

Figure 6. Surface normal concentration for different classes of polyps and folds.

be higher than that calculated for folds (see Fig. 6). In Fig. 6 it can be observed that the surface normal concentration offers a good discrimination between large polyps ($>= 10mm$) and all types of folds. This is very useful as the features discussed before were able to discriminate robustly only small/medium polyps while the discrimination for large polyps was less pronounced.

4. Classification

In order to assess the most robust classification scheme we have evaluated the performance of two different classifiers. The classifiers investigated are: the feature normalized nearest neighbor (FNNN) classifier [11] and the probabilistic neural network (PNN) classifier. We evaluated these classification schemes in order to determine their contribution to the reduction of false positives. In this implementation we have developed the *FNNN* classifier and tested its performance against established classification schemes, namely the *PNN* classifier.

Our *FNNN* training data consists of five polyps and five folds databases. During training we have segregated the polyps into small spherical, medium spherical, large spherical and elliptical. We also segregated the folds into small folds, small convex surface, medium folds and large folds. We have chosen to divide these databases by size in order to alleviate as much as possible the class overlap in the training stage. For training we have used 58 polyps and 247 folds.

5. Experiments and Results

In our tests we have used 57 patient datasets (prone and supine views) with 121 polyps, five patient data with 33 synthetic polyps and a phantom data with 47 polyps of various sizes. Overall sensitivities for real polyp detection were 72.73% and 66.12% when the *FNNN* and *PNN* classifiers were employed (see also Table 1). The false positive rates were 6.0, 4.7 for *FNNN* and *PNN* classifiers respectively. Sensitivities for polyps larger than 10mm were 100% (*FNNN*), 75% (*PNN*).

Table 1. Performance analysis for real polyp data

Type	Number	FNNN		PNN	
		TP	*Sen.*	*TP*	*Sen.*
$\geq 10mm$	4	4	100%	3	75%
$[5-10)mm$	25	23	92%	22	88%
$< 5mm$	79	52	65.82%	46	58.23%
Mass	11	7	63.67%	7	63.67%
Flat	2	2	100%	2	100%
Total	121	88	72.7%	80	66.16%
FP			6.0		4.7

When the *CAD-CTC* system has been applied to datasets with synthetic polyps, the overall sensitivities for *FNNN* and *PNN* classifiers were 84.85% and the false positives per dataset were 2.6, 3.0 respectively. Sensitivity for polyps larger than 5mm was 100% and sensitivity for polyps smaller than 5mm was 33.33% for both classifiers.

Table 2. Performance analysis for synthetic data

Type	Number	FNNN		PNN	
		TP	*Sen.*	*TP*	*Sen.*
$\geq 10mm$	9	9	100%	9	100%
$[5-10)mm$	17	17	100%	17	100%
$< 5mm$	6	2	33.33%	2	33.33%
Flat	1	0	00.00%	0	0%
Total	33	28	84.85%	28	84.85%
FP			2.6		3

For phantom data overall sensitivities were 89.36%, 85.10% when the *FNNN* and *PNN* classifiers were em-

ployed (see Table 3). Sensitivities for polyps $< 5mm$, 5 to 10*mm*, $>= 10mm$ and flat polyps were 100%, 100%, 100% and 44.44% for *FNNN* classifier. For *PNN* classifier the sensitivities in polyp detection were 92.85%, 92.74%, 100% and 44.44%.

To determine whether a polyp was correctly detected by the proposed *CAD-CTC* system, we cross-validated the detected polyps' location with the *CTC* reports prepared by the radiologists. Also we compared the results returned by the *CAD-CTC* system with the colonoscopy reports for supine and prone views. The average size of a typical interpolated CT dataset is 300MB and the processing time required by the algorithm to evaluate a dataset is 3.72 minutes when executed on a Pentium-IV 1.6GB PC with 1 GB memory.

Table 3. Performance analysis for phantom data

Type	Number	FNNN		PNN	
		TP	*Sen.*	*TP*	*Sen.*
$\geq 10mm$	14	14	100%	13	92.86%
$[5-10)mm$	19	19	100%	18	94.73%
$< 5mm$	5	5	100%	5	100%
Flat	9	4	44.44%	4	44.44%
Total	47	42	89.36%	40	85.10%
FP			4		0

6. Discussion and Conclusions

In this paper we propose four novel features that were successfully included in the development of an automated *CAD-CTC* system. The experimental data indicates that these features were efficient in discriminating polyps from folds as the algorithm demonstrated high sensitivity in polyp detection while maintaining a low level of false positive per dataset. Also in our experiments we evaluated two different classifiers in order to determine the optimal classification scheme that minimizes the false positive incidence. Our polyp detection technique was not designed for detection of flat polyps and small polyps adjacent to folds as their shapes resemble the characteristics of folds. To solve this problem we plan to develop a better surface detection technique in order to improve the segmentation of the polyps situated on folds. Also, approximately 11% of the false positives were generated by the residual material attached to the colonic wall. These false positives can be eliminated by employing texture analysis as they have a different density than the tissue that forms the colonic wall. It is useful to mention that our polyp detection technique outperforms the existing techniques [5,7] and in particular is very efficient in detecting medium ($>= 5mm$) and large ($>= 10mm$) polyps as these polyps are the most important clinical features. The experimental data indicated that the developed CAD polyp detection technique presented in this paper is a useful tool to be used in clinical studies.

7 Acknowledgments

We would like to acknowledge the contribution of our clinical partners in this project: Dr. Helen Fenlon (Department of Radiology) and Dr. Padraic MacMathuna (Gastrointestinal Unit) of the Mater Misericordiae Hospital, Dublin. This work was supported under an Investigator Programme Grant (02/IN1/1056) by Science Foundation Ireland (SFI).

References

[1] D.J. Vining, D.W. Gelfand, R.E. Bechtold, Technical feasibility of colon imaging with helical CT and virtual reality, AJR, vol. 162 pp. 104, 1994.

[2] C.D. Johnson, A.K. Hara, J.E. Reed, Virtual endoscopy: what's in a name?, AJR, vol. 171, pp. 1201-2, 1998.

[3] C.D. Johnson, A.K. Hara, CT colonography: the next colon screening examination?, Radiology, vol. 216, pp. 331-341, 2000.

[4] D.J. Vining, G.W. Hunt, D.K. Ahn, D.R. Stelts, P.F. Helmer, Computer-assisted detection of colon polyps and masses, Radiology, vol. 205, pp. 705, 1997.

[5] R.M. Summers, C.D. Johnson, L.M. Pusanik, J.D. Malley, A.M. Youssef, J.E. Reed, Automated polyp detection at CT colonography: Feasibility assessment in a human population, Radiology, vol. 219, pp. 51-59, 2001.

[6] H. Yoshida, Y. Masutani, P. MacEneaney, D. T. Rubin, A. H. Dachman, Computerized detection of colonic polyps at CT colonography on the basis of volumetric features: Pilot study, Radiology, vol. 222, pp. 327-336, 2002.

[7] D.S. Paik, C.F. Beaulieu, G.D. Rubin, B. Acar, R.B. Jeffrey, J. Yee, J. Dey, S. Napel, Surface normal overlap: a computer-aided detection algorithm with application to colonic polyps and lung nodules in helical CT, IEEE Trans Med Imaging, 23(6) pp. 661-75, 2004.

[8] G. Kiss, J. Cleynenbreugel, M. Thomeer, P. Suetens, G. Marchal, Computer-aided diagnosis in virtual colonography via combination of surface normal and sphere fitting methods, European Radiology, 12(1), pp. 77-81, 2002.

[9] R.C. Gonzalez, R.E. Woods, Digital image processing, Reading MA: Addison-Wesley, 1993.

[10] S.W. Zucker, R.A. Hummel, A Three-Dimensional edge operator, IEEE Transactions on Pattern Analysis and Machine Intelligence, 3(3), pp. 324-331, 1981.

[11] O. Ghita, P.F. Whelan, A bin picking system based on depth from focus, Machine Vision and Application, vol. 13, pp. 234-244, 2003.